



Activation volume and strain rate sensitivity in plastic deformation of nanocrystalline Ti



F. Wang^{a,*}, B. Li^b, T.T. Gao^a, P. Huang^b, K.W. Xu^b, T.J. Lu^{a,*}

^a State Key Laboratory for Mechanical Structure Strength and Vibration, Xi'an Jiaotong University, Xi'an, 710049, PR China

^b State Key Laboratory for Mechanical Behavior of Materials, Xi'an Jiaotong University, Xi'an, 710049, PR China

ARTICLE INFO

Available online 9 June 2012

Keywords:

Strain rate sensitivity
Activation volume
Nanocrystalline
Hexagonal close packed
Deformation mechanisms

ABSTRACT

The mechanical behavior of coarse grained, ultrafine grained and nanocrystalline Ti, which was fabricated on single crystalline Si substrate using a *d.c.* magnetron sputtering system, were investigated by nanoindentation tests at a range of strain rates; both the strain rate sensitivity and activation volume were obtained. It is demonstrated that the rate controlling mechanisms of plastic deformation for nanocrystalline Ti differ from those in coarse grained and ultrafine grained Ti. The implications of these findings for the mechanical properties of nanocrystalline hcp metals are also discussed.

© 2012 Elsevier B.V. All rights reserved.

1. Introduction

There is much current interest in the mechanical properties of nanocrystalline (NC) metals [1,2]. To shed light on the rate controlling deformation mechanism in NC metals, two activation parameters, i.e., strain rate sensitivity [3–6] and activation volume [6–8], were widely used to interpret the deformation kinetics which could provide insight into the deformation mechanisms.

Until very recently, only face-centered cubic (FCC) structure, notably Cu, Al and Ni, have been investigated in detail, whereas other crystal structures, have been studied to a far lesser degree in determination of the two parameters [9]. For FCC NC metals, the strain rate sensitivity of the flow stress was found to increase with reduced grain size [10,11] and this trend appears to hold independent of the processing routes and of the testing method employed. It was considered to be related to the transition of the deformation mechanism changing from dislocation mediated processes to grain boundary mediated processes [12]. However, the experimental results on grain size dependent strain rate sensitivity m and activation volume v in hexagonal close packed (HCP) metals are rather limited and controversial observations are still widely remained [10,11]. For example, Jia et al. indicated that the strain rate sensitivity of ultra-fine grained (UFG) Ti could drop by a factor of 2–3 compared with coarse grained (CG) Ti [13] while the inverse trend has been also reported [14]. Moreover, the dislocation mechanism of HCP metals is much complicated than those of FCC metals, for there are three glide modes including basal slip, prismatic slip and pyramidal slip. Therefore, it is still not clear how grain size affects the m of HCP metals, and systematic studies are needed to understand the strain

rate effect in HCP metals, especially when grain size enters nanoscale. In the present study, the strain rate sensitivity combined with apparent activation volume were quantitative evaluated by nanoindentation tests for CG, UFG and NC Ti, and the underlying deformation mechanisms were proposed and discussed.

2. Experimental details

Three Ti samples with various grain sizes were tested. One is CG Ti which was acquired from a commercial source. The CG Ti was etched in an electrolyte consisting of 100 ml H₂O, 2 ml HF and 5 ml HNO₃ to determine the grain size by optical microscopy. The UFG Ti was fabricated by Equal Channel Angular Pressing (ECAP) at room temperature from the CG Ti. The extruded billets of UFG Ti were 14.5 × 14.5 mm² in cross section and 80 mm in length. Another specimen is a Ti thin film deposited by dc magnetron sputtering on a single silicon wafer (100) using a high purity Ti target of 99.99% without substrate heating. The sputtering power and bias voltage were set as 200 W and –80 V, respectively. Then the grain microstructures of UFG and NC Ti samples were investigated by means of transmission electron microscope (TEM).

Nanoindentation experiments were performed on Nanoindenter XP® system (MTS, Inc) with a Berkovich diamond indenter over loading strain rate ranging from 0.001 to 0.2 s^{–1} at room temperature. For each sample, at least 8 effective sets of test data at each loading strain rate were used for subsequent analysis of hardness. The strain rate sensitivity and apparent activation volume were determined based on the derived nanoindentation hardness accordingly.

3. Results and discussion

The plan view optical image (Fig. 1a) shows the microstructure of as-received CG Ti sample. From a statistical analysis of grain size

* Corresponding authors.

E-mail addresses: wangfei@mail.xjtu.edu.cn (F. Wang), tjlu@mail.xjtu.edu.cn (T.J. Lu).

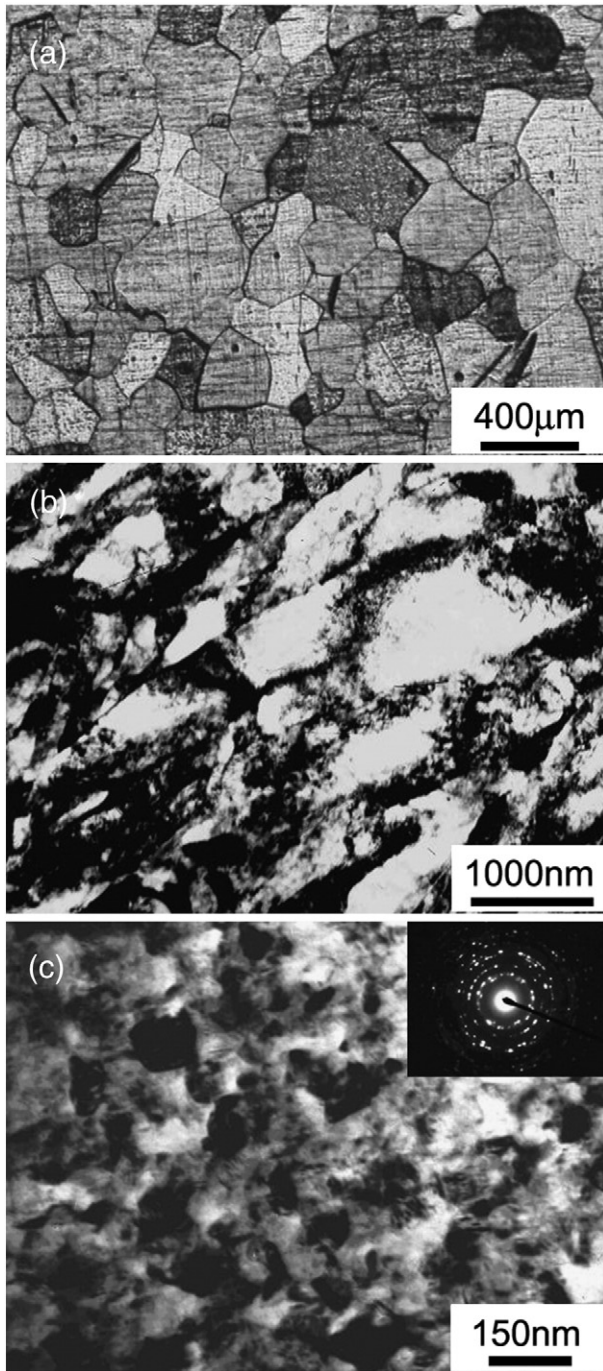


Fig. 1. (a) Optical micrograph of CG Ti in the as-received condition; (b) plan view TEM bright-field micrograph of UFG Ti; (c) plan view TEM bright-field micrograph of nc Ti as deposited, and the inset shows the selected area diffraction.

observed in the optical micrograph, the grain size of CG Ti was found to follow a lognormal distribution with an average value of $\sim 234 \mu\text{m}$. The representative plan view TEM bright-field micrograph (Fig. 1b) shows the microstructures of the UFG Ti. The grain size of the UFG Ti spread widely and exhibits elongated morphology having widths in a range of 200 nm–900 nm, and the average grain size for UFG Ti was about 340 nm estimated from a large number of TEM images of the UFG sample. In addition, Fig. 1c shows a representative planar-view TEM bright-field picture of the NC Ti. The corresponding electron diffraction patterns of the same area are shown in the inset of Fig. 1c. Further quantitative analysis of the planar-view grain size distribution derived from TEM observations yields an average grain size of $\sim 76 \text{ nm}$.

Fig. 2 shows the strain rate dependent hardness of the three Ti samples. The hardness of the NC Ti changes significantly as the strain rate is varied, while the UFG Ti shows relatively slighter but still pronounced discrepancy in hardness at various loading strain rates. In contrast, the CG Ti shows a negligible dependence of the hardness on strain rate. Despite those discrepancies, the hardness of all the Ti samples evaluated in present study increases with increasing indentation strain rate, indicating the flow stress of Ti exhibits positive strain rate sensitive.

In general, the strain rate sensitivity is defined as a variation of flow stress or hardness with applied strain rate and it can be derived from the equation [15]:

$$m = \frac{\partial \ln H}{\partial \ln \dot{\epsilon}} \quad (1)$$

where H is the hardness and $\dot{\epsilon}$ the applied strain rate. Then, strain rate sensitivity m shown in Fig. 2 was estimated from typical double logarithmic curve of hardness H versus indentation strain rate $\dot{\epsilon}$ according to Eq. (1). The strain rate sensitivity was found to be about 0.163, 0.067 and 0.007 for the NC, UFG and CG Ti, respectively. The variation of m exhibits a similar trend with fcc metals as the m increases when the grain size decreases to the ultra-fine and even nano scale.

In addition, the apparent activation volume V in indentation test can be calculated as

$$V = 3\sqrt{3}kT \left(\frac{\partial \ln \dot{\epsilon}}{\partial H} \right) \quad (2)$$

where k the Boltzmann constant and T the absolute temperature. Then the activation volume of the Ti specimens was obtained from the slope of linear fit of the H versus $\ln \dot{\epsilon}$ plots according to Eq. (2) as shown in Fig. 3. The magnitudes of V were estimated to be about 276, 57 and $5b^3$ for the CG, UFG and NC Ti respectively, where the b was assumed to be the Burgers vector of the prefer slip system $\{10\bar{1}0\}\langle 11\bar{2}0 \rangle$.

Despite some inconsistency in the absolute values which might be obtained using different synthesis or testing methods, as shown in Fig. 4, the grain size dependent strain rate sensitivity in present Ti samples shows a similar trend (indicated by the line in Fig. 4) with the variation trend in HCP metals reported in the literature [13,14,16–19]. For CG and UFG Ti, in general, forest dislocation is the primary short range barriers upon plastic deformation. In addition, as HCP metals lack of sufficient slip systems, CG and UFG Ti usually need twinning to accommodate plastic deformation, while twinning is rarely observed when its grain size enters nanoscale. For NC Ti, the extremely small apparent

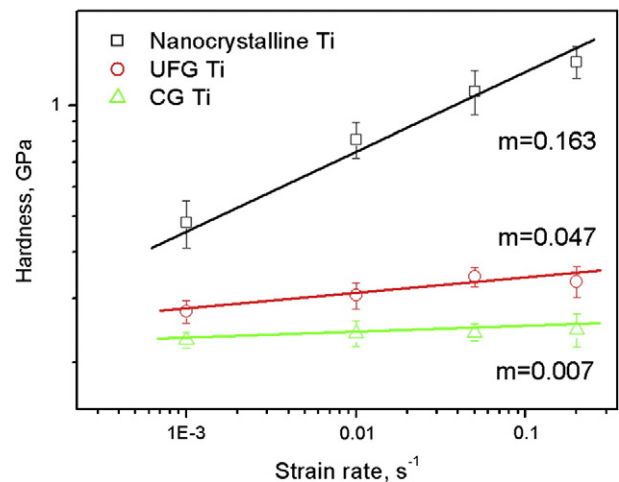


Fig. 2. Logarithmic plots of hardness as a function of indentation strain rate for Ti with different grain sizes.

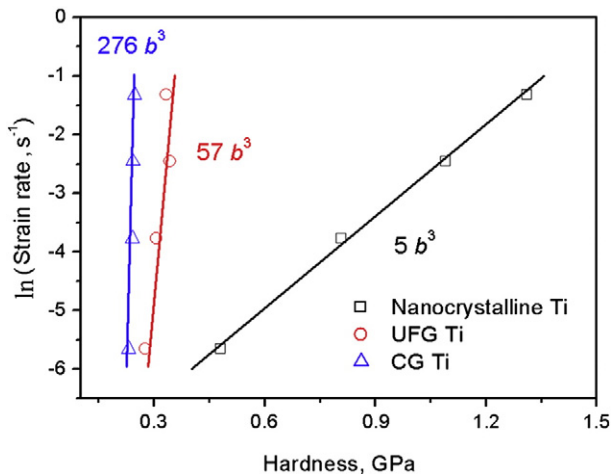


Fig. 3. Representative semi-log plot of $\ln(\dot{\epsilon})$ versus H for Ti with different grain sizes.

activation volume of $\sim 5b^3$ may indeed suggest the GB-related process attributes more while the grain size reduced from micron to nano scale. However, the magnitude of m for the NC Ti is estimated to be 0.163, which is still much smaller than the value expected for Coble creep ($m \sim 1$) or the value for grain boundary sliding ($m \sim 0.5$). These observations indicated Coble creep or grain boundary sliding are unlikely to be the sole dominant mechanism for the 76 nm grained NC Ti. Then, other possible mechanisms were considered as the candidate to be the rate controlling mechanism of the NC Ti sample in the following.

First, the probable rate controlling mechanisms might be that overcoming Peierls–Nabarro stress [16] as the apparent activation volume of NC Ti is only $\sim 5b^3$, which is similar to that of the nucleation of a kink pair for screw dislocations overcoming Peierls–Nabarro barriers. Then, the interactions between dislocation and grain boundary might also be the dominant mechanism. As grain size less than 100 nm, it is difficult for intra-grain dislocation sources to operate and leave little room for cross slip. However, the interactions between dislocation and grain boundary will become more active and important as the nanoscale grained Ti should possess high density of non-equilibrium grain boundaries with relatively larger number of grain boundary dislocation sources and pinning sites. Under this circumstance, the nucleation and annihilation of dislocations at the grain boundaries may become the rate controlling process rather than thermally activated motion of intra-grain dislocations in NC Ti [20]. The extremely small

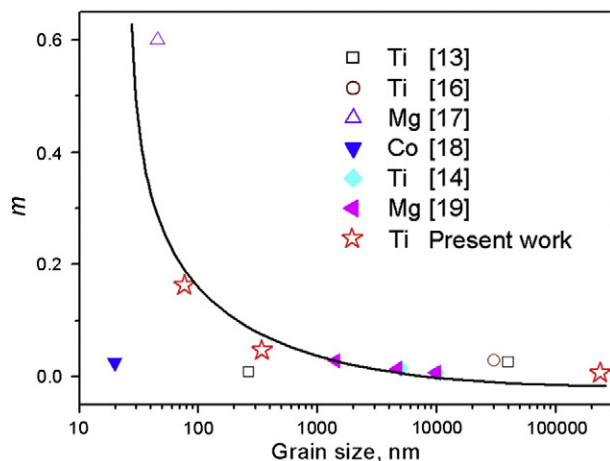


Fig. 4. Strain rate sensitivity of hcp metals as a function of grain size. The data point for CG Ti in this work (solid square) is marked by a horizontal right pointing arrow to show the grain size is off the scale of the plot.

apparent activation volume measured in the present NC Ti is consistent with that entailed by the interactions between dislocation and grain boundaries. For the CG Ti, however, the magnitudes of apparent activation volume is so large that the intersection of dislocation or the motion of jogs might be the rate controlling mechanism, as the activation volume value of both the two mechanisms is in the order of several hundred to a couple of thousand times b^3 .

4. Conclusions

Nanoindentation hardness tests were performed on CG, UFG and NC Ti, and the strain rate sensitivity and the apparent activation volume have been quantitatively determined accordingly. It is found that both the two activation parameters are strongly dependent on grain size, i.e., with decreasing grain size, the estimated strain rate sensitivity increases while the activation volume decreases. Moreover, by comparing the magnitudes of the two activation parameters with literature, Coble creep and grain boundary sliding were ruled out to be the dominant mechanism; and the mechanisms that overcoming the Peierls–Nabarro barrier and the interactions between dislocation and grain boundary was proposed to be the possible dominant mechanism for NC Ti. Furthermore, more thorough experimental examinations involving the effects of microstructure evolution and deformation modes on NC HCP metals are needed and already underway.

Acknowledgments

This work was supported by the National Basic Research Program of China (2010CB631002, 2011CB610306), the National Natural Science Foundation of China (51171141, 10825210), the National 111 Project of China (B06024), the Program for New Century Excellent Talents in University (NCET-11-0431), Xi'an Applied Materials Innovation Fund (XA-AM-201001) and the Fundamental Research Funds, for the Central Universities.

References

- [1] M.A. Meyers, A. Mishra, D.J. Benson, Prog. Mater. Sci. 51 (2006) 427.
- [2] T. Zhu, J. Li, Prog. Mater. Sci. 55 (2010) 710.
- [3] K. Jonnalagadda, N. Karanjgaokar, I. Chasiotis, J. Chee, D. Peroulis, Acta Mater. 58 (2010) 4674.
- [4] P. Huang, F. Wang, M. Xu, K.W. Xu, T.J. Lu, Acta Mater. 58 (2010) 5196.
- [5] F. Wang, P. Huang, K.W. Xu, Appl. Phys. Lett. 90 (2007) 161921.
- [6] R.J. Asaro, S. Suresh, Acta Mater. 53 (2005) 3369.
- [7] C.L. Wang, M. Zhang, T.G. Nieh, J. Phys. D Appl. Phys. 42 (2009) 115405.
- [8] F. Wang, P. Huang, T. Lu, J. Mater. Res. 24 (2009) 3277.
- [9] M. Dao, L. Lu, R.J. Asaro, J.T.M. De Hosson, E. Ma, Acta Mater. 55 (2007) 4041.
- [10] Q. Wei, J. Mater. Sci. 42 (2007) 1709.
- [11] Q. Wei, S. Cheng, K.T. Ramesh, E. Ma, Mater. Sci. Eng. A381 (2004) 71.
- [12] H. Conrad, Mater. Sci. Eng. A341 (2003) 216.
- [13] D. Jia, Y.M. Wang, K.T. Ramesh, E. Ma, Y.T. Zhu, R.Z. Valiev, Appl. Phys. Lett. 79 (2001) 611.
- [14] P. Cavaliere, Phys. B 403 (2008) 569.
- [15] J.R. Trelewicz, C.A. Schuh, Acta Mater. 55 (2007) 5948.
- [16] H. Conrad, High Strength Materials, John Wiley & Sons, New York, 1965.
- [17] S. Hwang, C. Nishimura, P.G. McCormick, Scr. Mater. 44 (2001) 1507.
- [18] Y.M. Wang, E. Ma, Appl. Phys. Lett. 85 (2004) 2750.
- [19] Q. Yang, A.K. Ghosh, Acta Mater. 54 (2006) 5159.
- [20] E.D. Tabachnikova, V.Z. Bengus, A.V. Podolskiy, S.N. Smirnov, V.D. Natsik, K. Csach, J. Miskuf, D.V. Gunderov, R. Valiev, Rev. Adv. Mater. Sci. 10 (2005) 229.